JPET Fast Forward. Published on April 15, 2009 as DOI: 10.1124/jpet.109.152967

JPET #152967

Discovery and Pharmacological Characterization of a Small Molecule Antagonist at Neuromedin U Receptor NMUR2

Jay J. Liu, Kemal Payza, Jian Huang, Ruifeng Liu, Tongming Chen, Martin Coupal, Jennifer M.A. Laird, Chang-Qing Cao, Joanne Butterworth, Stéphanie Lapointe, Malken Bayrakdarian, Shephali Trivedi, and J. Robert Bostwick

AstraZeneca Pharmaceutical LLP, CNS/Pain HTS Center, Wilmington, DE 19850, USA (J.J.L., J.H., R.L., T.C., S.T., J.R.B.), and AstraZeneca R&D Montreal, Montreal, Quebec, Canada H4S 1Z9 (K.P., M.C., J.M.A.L., C.Q.C., J.B., S.L., M.B.)

JPET #152967

Running Title: NMUR2 antagonist

Correspondence author:
Jay Liu, Ph.D.
AstraZeneca Pharmaceutical LLP, CRDL C253H
1800 Concord Pike, Wilmington, DE 19850-5437
Tel. 302-886-2667
FAX. 302-886-1502
E-mail: jay.liu@astrazeneca.com

Contents:

31 text pages
6 figures
2 tables
29 references
235 words in Abstract
744 words in Introduction
926 words in Discussion

Abbreviations:

NMU, neuromedin U; NMS, neuromedin S; GPCR, G protein-coupled receptor; CNS, central nervous system; ECL, electrochemiluminescent; FCA, Freund's complete adjuvant; HTS, high throughput screen; FLIPR, fluorometric imaging plate reader; PI, phosphoinositide; CRH, corticotrophin-releasing hormone; GI, gastrointestinal; SCN, suprachiasmatic nucleus; PVN, paraventricular nuclei; BSA, bovine serum albumin; R-PSOP, (R)-5'-(Phenylaminocarbonylamino)spiro[1-azabicyclo[2.2.2]octane-3,2'(3'H)-furo[2,3-b]pyridine].

Recommended Section

Neuropharmacology

ABSTRACT

Neuromedin U, through its cognate receptor NMUR2 in the central nervous system, regulates several important physiological functions including energy balance, stress response and nociception. By random screening of our corporate compound collection with a ligand binding assay, we discovered R-PSOP, a highly potent and selective NMUR2 antagonist. R-PSOP is a nonpeptidic small molecule with a chemical composition of $C_{20}N_4O_2H_{22}$. In competition binding experiments, this compound was found to bind to NMUR2 with high affinity; the K_i values were determined to be 52 and 32 nM for the human and rat NMUR2, respectively. Moreover, in functional assays measuring phosphoinositide turnover or intracellular calcium mobilization, R-PSOP strongly inhibited the responses stimulated by peptide agonists NMU-25, NMU-23 and NMU-8 in HEK293 cells expressing NMUR2. From Schild analyses, the functional K_b values for R-PSOP were determined to be 92 and 155 nM at human and rat NMUR2, respectively. Highly selective for NMUR2, R-PSOP exhibited low affinity to the other subtype of NMU receptor, NMUR1, with a K_i value >10 μM. R-PSOP *in vivo* attenuated NMU-23-evoked nociceptive responses in a rat spinal reflex preparation. To our knowledge, this is the first antagonist ever reported for NMU receptors. This compound could serve as a valuable tool for further understanding the physiological and pathophysiological roles of NMU system, while providing a chemical starting point which may lead to development of new therapeutics for treatment of eating disorders, obesity, pain and stress-related disorders.

Introduction

Neuromedin U (NMU) is a brain-gut peptide originally isolated from porcine spinal cord and named for its activity to contract rat uterine smooth muscle (Minamino et al., 1985). NMU has now been found in almost all vertebrate species and implicated in a wide variety of physiological processes, such as energy homeostasis, nociception, stress, inflammation, reproduction, bone remodeling, and cardiovascular and gastrointestinal (GI) functions (Brighton et al., 2004). Different molecular forms of NMU have been identified in various species: the 25-mer (NMU-25) in human and pig, the 23-mer (NMU-23) in rodents, and NMU-8 among other species. These peptides have similar biological activity and share a common C-terminal 7-amino acid segment, which is essential for biological activity. NMU is widely distributed in the body, with the highest abundance in the central nervous system (CNS), adrenal gland, GI and genitourinary tract (Domin et al., 1987; Ballesta et al., 1988). Recently, a 36-mer peptide, neuromedin S (NMS), was identified in rat brain. Its structure and biological activity is similar to NMU, but it is exclusively expressed in suprachiasmatic nucleus (SCN) in the brain and in testes and spleen at the periphery (Mori et al., 2005; Vigo et al., 2007). NMS acts at the same receptors as NMU and may play a role in the mammalian circadian oscillator system.

Two high affinity receptors, NMUR1 and NMUR2, have been identified for NMU and NMS. They are G protein-coupled receptors (GPCR) formerly known as “orphan” receptor FM3/GPR66 and FM4 (Fujii et al., 2000; Howard et al., 2000; Raddatz et al., 2000). The tissue distribution of the two receptors is quite distinct, yet complementary to each other. The expression of NMUR1 appears to be confined to peripheral tissues, particularly the GI tract, pancreas, uterus and testes (Fujii et al., 2000). NMUR2, in contrast, is predominantly expressed

in the CNS, with the highest level in the arcuate and paraventricular nuclei (PVN) of the hypothalamus, nuclei accumbens, hippocampus, thalamus, medulla oblongata and spinal cord (Guan et al., 2001).

Over the past several years, significant progress has been made towards understanding the mechanisms and physiological roles of NMU system. It is increasingly clear that NMUR2 mediates the central effects of NMU for the regulation of food intake, energy balance, stress response and nociception. In the brain, NMUR2 is prominent in the hypothalamic regions known to be associated with regulation of food intake and energy balance. Acute central administration of NMU suppresses food intake and increases energy expenditure in rodents (Howard et al., 2000). Long-term NMU treatment reduces body weight and adiposity in mice. Genetic ablation of NMUR2 abolishes the effects of both acute and chronic central NMU injection on food intake and body weight in mice (Zeng et al., 2006; Egecioglu et al., 2009). The high level NMUR2 expression in PVN, a major site for corticotrophin-releasing hormone (CRH) release, also suggests that NMU system may play a role in mediating stress responses. Indeed, NMU stimulates CRH release from hypothalamic explants *in vitro*, and direct NMU administration into PVN significantly elevates plasma ACTH and corticosterone level in rodents (Thompson et al., 2004). Central NMU injection induces stress-related behaviors (Hanada et al., 2001). Conversely, NMU-knockout mice exhibit blunted behavioral response to environmental stress (Nakahara et al., 2004). NMU and NMUR2 are also abundantly expressed in nociceptive sensory pathways, including spinal dorsal horn, dorsal root ganglia, thalamus and brain stem (Cao et al., 2003; Yu et al., 2003). Acute spinal or supraspinal NMU administration increases pain sensitivity in rodents. NMUR2-null mice exhibit reduced pain sensitivity in hot plate and formalin test (Zeng et al., 2006; Torres et al., 2007).

Based on its physiological roles, NMUR2 receptor has been proposed to be a potential target for developing new therapeutics for treatment of eating disorders, obesity, stress-related disorders and pain. However, the existing NMU analogs, antibodies and SiRNAs have limited clinical value due to their poor pharmacokinetic properties. Extensive efforts to generate a CNS-penetrable small molecule agonist or antagonist at NMUR2 (or NMUR1) by peptidomimetic approaches have been unsuccessful thus far.

In this article, we describe the identification of a highly potent and selective small molecule NMUR2 antagonist by screening our corporate compound collection using a novel electrochemiluminescent (ECL) ligand binding assay. We characterized the pharmacological properties of this first ever-reported NMUR2 antagonist and demonstrated its potential as a tool compound for further understanding the physiological/pathophysiological roles of NMU system and as a chemical starting point that may lead to development of new therapeutics for a number of CNS disorders.

JPET Fast Forward. Published on April 15, 2009 as DOI: 10.1124/jpet.109.152967
This article has not been copyedited and formatted. The final version may differ from this version.

Methods

Materials and instruments.

NMU-8, NMU-23, human NMU-25, bovine serum albumin (BSA), probenecid, EGTA, HEPES and Freund's complete adjuvant (FCA) were purchased from Sigma Aldrich (St. Louis, MO). Nonwash calcium assay kit and fluorometric imaging plate reader (FLIPR) were products from Molecular Devices, Inc (Sunnyvale, CA). $Ru(bpy)_3^{2+}$-NMU23 and MSD Multi-Array™ High Bind 384-well black plates were custom made by MSD, Inc. (Gaithesburg, MD). Meso Scale Discovery Sector HTS reader and ECL assay kit were also from MSD, Inc. [^{3}H]*myo*-inositol, [^{125}I]NMU-25 and WGA-coated PVT SPA beads were purchased from Amersham GE Healthcare (Piscataway, NJ). The compound 5'-(Phenylaminocarbonylamino)spiro[1-azabicyclo[2.2.2]octane-3,2'(3'H)-furo[2,3-b]pyridine] (PSOP) and its two enantiomers, R-PSOP and S-PSOP, were prepared according to the experimental procedure described in the patent application WO1999003859.

Cell culture and membrane preparation.

HEK293S cells stably transfected with NMUR1 or NMUR2 (human and rat) were cultured in DMEM supplemented with 10% fetal bovine serum and 0.25 mg/ml hygromycin and maintained at 37 ^oC in a CO_2 incubator. For membrane preparation, the cells were harvested and resuspended in lysis buffer (50 mM Tris, pH 7.0, 2.5 mM EDTA, 0.5 mM PMSF) at 5 x 10^6 cells/ml. Cells were then homogenized with a Polytron and centrifuged at 1000g for 10 min at 4°C. Supernatants were centrifuged at 46,000g for 30 min. Membrane pellets were resuspended in membrane buffer (50 mM Tris-HCl, 0.32 M sucrose, pH 7.0), aliquoted, and frozen in dry

ice/ethanol and stored at -70°C until use. The protein concentration was determined by Bradford method using BSA as the standard (Bradford, 1983).

ECL ligand binding assay and high throughput screening (HTS).

ECL membrane binding assay was carried out according to the instructions of the assay kit from MSD, Inc.. Briefly, NMUR2 membranes were diluted in assay buffer (25 mM HEPES, 5 mM $MgCl_2$, 1 mM $CaCl_2$, pH 7.4) and dispensed at 1 μg protein/well in 2 μl into assay plates (MSD Multi-array™ High Bind 384-well black wall). The immobilization of the receptors to the bottom surfaces of the plates occurred when plates were incubated at room temperature for 1 hr. 13 μl of a blocking agent (containing BSA) was added to minimize non-specific binding. After addition of test compounds to each well, $Ru(bpy)_3^{2+}$-NMU-23 was added to the assay plates to start the binding reaction. Plates were incubated at room temperature for 1 hr. At the end of the incubation, Reading Buffer from the assay kit containing tripropylamine was added to each well and the ECL readings were immediately taken on Sector HTS reader. The total reaction volume of the binding reaction was 25 μl/well, and the final labeled ligand concentration was 0.5 nM.

To eliminate false positives from color quenching and chemical reactivity, the active samples were counter-screened in an assay measuring the binding of biotinylated $Ru(bpy)_3^{2+}$-IgG to the surface of avidin-coated plates.

[^{125}I] NMU-25 competition binding.

Cell membranes containing NMU receptors were diluted in binding buffer (25 mM HEPES, pH 7.4, 5 mM $MgCl_2$, 1 mM $CaCl_2$, 0.2% BSA) and incubated with WGA-coated SPA beads for 1 hr on ice. The mixture of membranes and SPA was dispensed into each well of a 96-well white opaque plate containing test compounds or peptides in binding buffer. After addition

JPET Fast Forward. Published on April 15, 2009 as DOI: 10.1124/jpet.109.152967
This article has not been copyedited and formatted. The final version may differ from this version.

of [^{125}I] NMU-25, the plate was put on a shaker and incubated at room temperature for 1 hr. The radioactivities of the bound ligand were measured by a Topcount Reader. Non-specific binding was defined by the binding in the presence of 1 μM NMU-8.

Intracellular calcium mobilization.

HEK293S cells stably expressing NMU receptors were plated onto a poly-D-lysine coated 384-well black plate with clear bottom. After overnight culture, the cells were loaded with nonwash calcium-sensitive fluorescent dye (in calcium 4 assay kit from Molecular Devices, Inc.) for 30 min and incubated with test compounds in Hanks buffer for 15 min. The plate was then transferred onto a FLIPR and the peptide agonist was applied to the cells. The fluorescence response, as an indicator of changes in intracellular calcium concentration triggered by agonist stimulation, was recorded with excitation wavelength at 488 nm and emission wavelength at 510 nm, and the data were analyzed by FLIPR software.

Phosphoinositide turnover.

HEK293S cells expressing NMUR2 receptor were plated onto 24-well plates and grown in medium containing 5 μCi/ml [^{3}H]*myo*-inositol for 2 days. After removal of the medium, the cells were pre-incubated with test compounds in Hanks buffer containing 10 mM LiCl for 10 min. The peptide agonist was added to each well and the plate was incubated at 37 ^{o}C for 45 min. The amount of [^{3}H]inositol phosphate that accumulated in the cells, as a result of the stimulated phosphoinositide turnover, was measured by an ion exchange column chromatography method, as described previously (Liu et al., 2003).

Broad *in vitro* pharmacological selectivity profiling.

R-PSOP was evaluated *in vitro* for its activities at a broad spectrum of biological targets, including receptors, ion channels, enzymes and transporters. The studies were mainly performed in MDS Pharma Service, Inc. (Ontario, Canada) and BioSignal, Inc (a subsidiary of PerkinElmer, Boston, MA) using standard methods and assay conditions according to the literature and as described on the websites of the two outsourcing companies.

***In vivo* studies.**

In vivo studies on nociceptive responses were carried out on adult male Sprague-Dawley rats (Charles River, St. Constant, QC, Canada) by experimenters blind to the treatment the animals received. All experiments were approved by the AstraZeneca R&D Montréal Animal Care Committee in accordance with the Canadian Council on Animal Care (CCAC) and the Association for the Assessment and Accreditation of Laboratory Animal Care (AAALAC) guidelines. Rats were tested naïve or 24 hr after intraplantar injection of FCA into one hind paw.

The heat sensitivity of the plantar surface of the paw was assessed as previously described (Yu et al., 2003). Briefly, rats were placed on a transparent plastic enclosure on a glass surface maintained at 30°C and habituated for at least 30 minutes. The pain thresholds were measured using a radiant heat source connected to an automatic timer. When the hind paw was lifted, the heat automatically shut off and the latency was recorded. Two readings were taken at 5 min intervals. The cutoff time of 20 seconds was established to prevent tissue injury. R-PSOP in 10 μl saline was delivered by intrathecal injection under brief isoflurane anesthesia.

Electrophysiological recording of flexor reflex responses were performed as previously described (Yu et al., 2003). Briefly, extracellular recordings of flexor α-motoneuron activity

were made from a filament of the nerve to the posterior biceps femoris-semitendinosus muscles in decerebrate-spinal rats. The excitability of the flexor reflex was determined by measuring efferent activities evoked by touch, pinch and heat (water 52 °C) stimuli applied to the hind paw. Drugs were delivered via an intrathecal cannula in a volume of 10 µl, followed by a 10 µl saline flush.

Pharmacokinetic profiling.

R-PSOP was dissolved in saline and administered to adult male Sprague-Dawley rats via oral or intravenous *(i.v.)* route. Blood samples were collected at different time points post-dosing (5 min to 11 hr) and the plasma was isolated by centrifugation. Plasma proteins were precipitated with cold acetonitrile containing 0.1% formic acid. Following centrifugation R-PSOP in the resulting supernatants was quantitated by HPLC-mass spectrometry. The pharmacokinetic parameters of R-PSOP were estimated using standard non-compartmental methods. For measurement of CNS penetration, the rats were sacrificed after *i.v.* dosing, and the distribution of R-PSOP in the brain, spinal cord and plasma was analyzed by HPLC-mass spectrometry.

Data analysis.

HTS data were analyzed with ActivityBase (IDBS, Inc., Guildford, UK) and Spotfire (TIBCO, Somerville, MA) software. The Z'-factor, as an indicator of assay performance in a HTS setting, was calculated based on the method described in literature (Zhang et al., 1999). The binding K_d, K_i and functional K_b values were calculated using GraphPad Prism (GraphPad Software Inc., San Diego, CA). The statistical analyses of *in vivo* data were also performed with GraphPad Prism.

Results

ECL Ligand Binding Assay and HTS.

Radioligand binding assay is a sensitive and reliable technology for detection of compounds that act at membrane receptors. However, the utility of a radioactive assay in a large scale HTS is limited due to safety and waste concerns. Several non-radioactive alternatives have been developed. Among them, ECL is the simplest homogeneous (nonseparation) method with sensitivity comparable to the radioactive assays. The principle and applications of ECL technology have been thoroughly described elsewhere (Marquette and Blum, 2008; Miao, 2008). To establish an ECL binding assay for NMUR2 receptor, the peptide NMU-23 was labeled at the N-terminus with $Ru(bpy)_3^{2+}$ and allowed to bind to the human NMUR2 receptor in the cell membranes immobilized on the electrode on the bottom of each assay plate. Upon application of an electric current, the receptor-bound $Ru(bpy)_3^{2+}$-ligand undergoes an oxidation-reduction cycle in the presence of a co-reactant tripropylamine and emits light. Signal is only generated when the $Ru(bpy)_3^{2+}$ label is in close proximity to the electrode, thus discriminating the bound label from the unbound and enabling a no wash, homogenous assay format. In this assay the active compounds that compete with $Ru(bpy)_3^{2+}$-NMU23 for binding to NMUR2 would be detected by the decrease in ECL intensity.

Figure 1 shows the structure of the ligand, $Ru(bpy)_3^{2+}$-NMU23, the saturation and competition binding curves from the ECL assay on human NMUR2. From the saturation binding experiment, the K_d value and the total number of binding sites (B_{max}) were determined to be 0.8 nM and 4 pmol/mg membrane protein, respectively. From competition binding experiments, the K_i values for NMU-25 (human), NMU-23 and NMU-8 (porcine) were

JPET Fast Forward. Published on April 15, 2009 as DOI: 10.1124/jpet.109.152967
This article has not been copyedited and formatted. The final version may differ from this version.

determined to be 3.2, 4.7 and 3.0 nM, respectively. The K_i values from ECL assay for were very close to those derived from a parallel radioactive binding assay with [^{125}I] NMU-25 (reported below) and in general agreement with literature (Hosoya et al., 2000; Howard et al., 2000; Kojima et al., 2000; Raddatz et al., 2000; Shan et al., 2000; Szekeres et al., 2000).

The ECL-based NMUR2 binding assay was used to screen our corporate compound collection. Approximately 670,000 compounds with diverse structures were tested at 10 μM for their ability to displace the binding of 0.5 nM $Ru(bpy)_3^{2+}$-NMU23 to human NMUR2 receptors. The assay performance was strong during the entire HTS, with a signal/background window >11 and a Z'-factor >0.7. Figure 2a shows the scattergram of the data from a typical 384-well plate. A total of 355 compounds showed activities >50% and were identified as putative hits. After re-test in triplicates, 57 hits were confirmed. Among them, the most active compound was 5'-(phenylamino-carbonylamino)spiro[1-azabicyclo[2.2.2]octane-3,2'(3'H)-furo[2,3-b]pyridine], which was given a generic name as PSOP. PSOP is a nonpeptidic small molecule with a chemical composition of $C_{20}N_4O_2H_{22}$. Since PSOP is racemic, the two enantiomers of PSOP were synthesized, and their binding affinities at NMUR2 were evaluated. R-PSOP was found to be the active enantiomer, whereas S-PSOP was completely inactive. The structures of PSOP (upper) and R-PSOP (lower) are shown in Figure 2b.

High Affinity Binding of R-PSOP to NMUR2.

The affinities of R-PSOP binding to human and rat NMUR2 were evaluated in both ECL and radioactive membrane binding assays, and similar results were obtained from the two different assays. Figure 3 shows that R-PSOP inhibits the binding of [^{125}I] NMU-25 to human NMUR2 membranes in a concentration-dependent manner and with a Hill coefficient close to

JPET Fast Forward. Published on April 15, 2009 as DOI: 10.1124/jpet.109.152967
This article has not been copyedited and formatted. The final version may differ from this version.

unity, suggesting that R-PSOP binds competitively to the same site on the receptor as NMU-25. From radioactive competition binding assays, the K_i values were determined to be 52 and 32 nM for the human and rat NMUR2, respectively. The reference peptide, NMU-8, had K_i values at 3 and 4.4 nM in the same assay. From ECL binding assay, similar K_i values were obtained for R-PSOP binding to human and rat NMUR2 (78 and 44 nM, respectively).

Functional Antagonist Activity of R-PSOP at NMUR2.

Through the $G_{q/11}$ signaling pathway NMU stimulates the classical response of PI turnover and intracellular calcium mobilization in HEK293 cells expressing NMUR2. Pretreatment of the cells with R-PSOP strongly inhibited the second messenger response induced by agonist NMU-25, NMU-23 or NMU-8, although the compound itself has no intrinsic agonist activity in either PI turnover or intracellular calcium mobilization assay.

As shown in Figure 4, R-PSOP concentration-dependently inhibited the PI turnover response in human NMUR2-expressing cells stimulated by 10 nM NMU-25 (EC_{50} ~5 nM). The IC_{50} value was determined to be 86 nM (n=2). At 1 μM, R-PSOP completely blocked the agonist response. In a separate experiment, it was found that R-PSOP treatment had no significant effect on the basal level of PI turnover in the cells treated with LiCl, indicating that R-PSOP did not have inverse agonist activity, rather, it behaved as a pure antagonist at NMUR2.

To further characterize the mode of action, we performed Schild analysis on the effects of R-PSOP on the intracellular calcium mobilization response induced by NMU-25 in HEK293 cells expressing human or rat NMUR2. The response was measured by FLIPR using a calcium-sensitive dye. Figure 5A shows the curves of the agonist concentration-dependent response in the presence of increasing concentrations of R-PSOP. As the concentration of the inhibitor

increases, the curves were parallel shifted to the right, consistent with a competitive mode of inhibition. From Schild analysis (Fig. 5B), the K_b values were calculated to be 92 and 155 nM at human and rat NMUR2, respectively.

A 5-min wash of the cells with Hanks buffer after R-PSOP treatment almost completely restored the agonist-induced response, suggesting that the interaction of this antagonist with NMUR2 is reversible as well as competitive.

Selectivity of R-PSOP at NMUR2 over Other Biological Targets.

For selectivity evaluation, PSOP and R-PSOP was tested at the other subtype of NMU receptor, NMUR1, in [^{125}I] NMU-25 binding assay. The binding activity of PSOP and R-PSOP was very weak at both human and rat NMUR1, each with a K_i value >10 μM. Moreover, in NMUR1 functional assay PSOP and R-PSOP were inactive at concentrations up to 10 μM in inducing calcium mobilization response or inhibiting the response induced by NMU-23. The data indicate that R-PSOP has a >200-fold selectivity at NMUR2 over NMUR1.

In addition, R-PSOP was tested *in vitro* for activities at a panel of over 100 various biological targets including receptors, ion channels, transporters and enzymes. R-PSOP was inactive at all the targets, except the ionotropic 5-HT3 and α7 nicotinic receptors. R-PSOP bound to human 5-HT3 and α7 receptors with K_i values at 220 and 460 nM, respectively, and activated the channels at >5 μM concentrations. The racemic compound, PSOP, showed a similar activity. Table 1 provides an abbreviated list of the targets tested, the assays used and the activities of R-PSOP in those assays. A complete list is also provided in the Supplemental Data file. Overall, R-PSOP has a reasonably clean *in vitro* pharmacological profile.

Physicochemical and pharmacokinetic properties of R-PSOP.

To assess the usefulness of R-PSOP as a tool compound for *in vivo* studies, we have evaluated its physicochemical and pharmacokinetic properties. R-PSOP has a molecular weight of 350 and excellent physicochemical properties: polar surface area 67 A^2, logP 2.2, logD (pH7.4) 0.99 and aqueous solubility 6.5 mM. The intrinsic clearance was low; 8 and 13 µl/min/mg when measured with human and rat liver microsomal preparations. R-PSOP also showed good permeability in CaCo2 assays with A to B P_{app} at 3 and B to A P_{app} at 5.6 µM·cm/sec at pH7.4, respectively. Pharmacokinetic evaluation of R-PSOP in rats (Table 2) indicated that R-PSOP had low oral bioavailability, moderate half-life and high clearance. The CNS penetration of PSOP was moderate, as evidenced by the brain/plasma ratio of approximately 0.2 and spinal cord/plasma ratio of approximately 0.4. The physicochemical and pharmacokinetic properties of R-PSOP support its utility *in vivo* for interrogating the effects of NMUR2 inhibition in animal models.

***In vivo* effect of R-PSOP on nociceptive responses evoked by NMU-23 or by paw inflammation.**

To establish whether R-PSOP acted as a functional antagonist of NMUR2 in their native environment, we tested R-PSOP *in vivo* on spinal nociceptive reflexes, since NMUR2 are expressed by intrinsic neurons in spinal cord. As reported previously (Yu et al., 2003), NMU-23 applied to the surface of the spinal cord via an intrathecal cannula in a decerebrate spinalized rat preparation increased nociceptive spinal reflex responses to pinch of the paw. R-PSOP injected intrathecally in this preparation 15 min after NMU-23 application significantly attenuated the enhanced responses to pinch (Figure 6). A similar attenuation of enhanced responses to touch of the paw was also observed. When R-PSOP was given intrathecally in the absence of NMU

pretreatment, it had no effect on the reflex responses, suggesting there is no NMU tone in the rat spinal cord under normal conditions (Figure 6).

We further assessed the effect of R-PSOP given intrathecally in rats with acute paw inflammation induced by FCA, both electrophysiologically and behaviorally. R-PSOP had no marked effect on the enhanced reflex responses to pinch, touch or heat in FCA-treated rats. Likewise, R-PSOP had no effects on the reflex withdrawal latency to heat stimuli applied to the paw in awake, intact rats. There was no significant difference in response latency to a standard heat stimulus between vehicle treated rats (latency 7.0 ± 0.4 sec, n = 7) and those treated with 5 nmol R-PSOP in 10 μl saline (latency 6.9 ± 0.4 sec, n = 7). These data suggest that there is no elevated NMU tone in the rat spinal cord induced by acute inflammation.

Taken together, we have identified R-PSOP from HTS and demonstrated that it is a highly potent and selective NMUR2 antagonist. This compound binds competitively to NMUR2 with high affinity, and it reversibly blocks the activation of the receptor by peptide agonist. R-PSOP also acts as a functional antagonist *in vivo* attenuating NMUR2-mediated nociceptive responses.

JPET Fast Forward. Published on April 15, 2009 as DOI: 10.1124/jpet.109.152967
This article has not been copyedited and formatted. The final version may differ from this version.

Discussion

A sensitive and HTS-compatible non-radioactive homogeneous ligand binding assay for membrane receptors, especially GPCRs, has always been challenging. Using the ECL technology, we developed a HTS assay to screen for compounds that bind to NMUR2 receptors. The assay is simple, fast and highly sensitive. The major caveat in the use of this assay technology is the interference produced by compounds with strong colors or high oxidation-reduction potential. This shortcoming can be overcome by counter-screening with biotinylated $Ru(bpy)_3^{2+}$-IgG binding to avidin-coated plates. In addition, since the labeled ligand starts to dissociate from the receptor upon addition of the Reading Buffer, the plate reading has to be made within an inconvenient short time frame of 2 min. Nonetheless, a HTS campaign was successfully completed with the ECL membrane binding assay, and a highly potent compound, R-PSOP, was discovered.

The binding of R-PSOP to NMUR2 appears to be competitive with NMU-25 and NMU-23. It is possible that R-PSOP binds to the same or overlapping site as the peptide agonist. Comparing the structure of R-PSOP with the highly conserved C-terminal 7-amino acid segment of NMU peptide, there are two apparent common features that may be critical for receptor binding: a positively charged amine group and a lipophilic aromatic group. The tertiary amine group in the azabicyclic octane ring and the terminal phenyl group in R-PSOP could correspond to the arginine and phenalanine residues, respectively, in the peptide. Similar compounds without the phenyl group were inactive in the binding assay. Correspondingly, changing the phenalanine residue destroys the activity of the peptide (Brighton et al., 2004). The amphiphilic nature of the ligand-binding site is corroborated by the structures of two recently disclosed non-

selective small molecule NMUR agonists, (2-(trityloxy)ethyl)guanidine and (3-(trityloxy)propyl)guanidine. It was reported that when the guanidine group was replaced by non-basic substituents, such as 2-(thiophen-2-yl)ethanyl and 2-(pyridin-4-yl)ethanyl, the bioactivity of the resulting compounds was lost (Meng et al., 2008).

The binding site for peptide agonist is generally believed to be well-conserved between NMUR1 and NMUR2. It is surprising that R-PSOP achieves more than >200-fold selectivity at NMUR2 over NMUR1, while binding to the same site as the peptide agonist. Sequence alignment and molecular modeling based on the known GPCR crystal structures might provide insight into mechanisms of R-PSOP interaction with NMUR2 and the subtype selectivity. Site-directed mutagenesis could also help pinpoint the residues on the receptor responsible for the selectivity. It is likely that some steric hinderance from certain divergent residues on NMUR1 prevents R-PSOP from reaching the binding pocket. Even though R-PSOP *per se* is inactive at NMUR1, it might be possible to generate NMUR1-active compounds by modifying the structure of R-PSOP. Indeed, R-PSOP could be the chemical starting point for development of compounds with various pharmacological properties, including agonists, antagonists or inverse agonist, at NMUR1 and NMUR2.

R-PSOP has no intrinsic agonist or inverse agonist activity at NMUR2. Most likely it exerts its effect by simply blocking the natural agonist from reaching to the binding pocket of the receptor, thus preventing receptor activation. Therefore, the effects of R-PSOP *in vivo* on various physiological processes are very likely to be dependent on the tone of the NMU system involved. The results we observed in the nociceptive system reinforce this hypothesis. Thus R-PSOP had no effect on nociceptive responses when given intrathecally either in normal, naïve rats, or in animals with an acute inflammation of the paw. In contrast, R-PSOP was effective at

attenuating the effects of exogenously applied NMU in the same system, indicating that it reached the spinal neurons expressing NMUR2 receptors. The reversal of the effects of NMU was not complete, likely due to failure to block the effects on NMUR1, which is also expressed in the pain pathway in the spinal cord, although on a different cell type, primary afferent terminals (Yu et al., 2003).

NMU and its receptors have been implicated in an ever-increasing number of physiological processes, including food intake, energy balance, stress response, inflammation, nociception, circadian rhythms, reproduction, and GI and cardiovascular functions (Brighton et al., 2004). In general, three lines of evidence have been used to support the claims: tissue distribution data, the pharmacological effects of peptides and the phenotypes of genetically modified animals. However, exogenously applied NMU peptide may not reflect true physiological conditions, and the phenotypic analysis of knockout mice might be limited by gene compensation and developmental effects. Potent and selective antagonists at NMU receptors, such as R-PSOP, will provide pharmacological tools to elucidate further the physiological and pathophysiological roles of NMU system.

NMUR2 has been proposed to be a drug target for developing new therapeutics for several major unmet medical needs (Howard et al., 2000; Guan et al., 2001; Brighton et al., 2004; Sato et al., 2007). For example, NMUR2 agonists could potentially be used to treat obesity and metabolic disorders, whereas NMUR2 antagonists were hypothesized to be beneficial for anorexia, chronic pain, osteoporosis and stress-related disorders. The discovery of R-PSOP as a potent and selective antagonist at NMUR2 represents a breakthrough towards the realization of the potential of NMUR2 as a drug target. Further evaluation of the effects of

systemic or local administration of R-PSOP or its improved analogs in various animal models will help address many unanswered questions and provide insight into future directions.

In conclusion, we have identified from HTS a highly potent and selective NMUR2 antagonist. This compound could be a valuable tool for further understanding the physiological and pathophysiological roles of the NMU system and provides a chemical starting point that may lead to development of new therapeutics for a number of CNS disorders.

Acknowledgements

We thank Dr. Manon Valiquette for providing all the cell lines, Dr. Clay Scott, Dr. James Campbell, Kenneth Mitchell, Dr. Norman Ledonne and Linda Sygowski for critically reading the manuscript and fruitful discussions.

References

Ballesta J, Carlei F., Bishop AE, Steel JH, Gibson SJ and Fahey M (1988) Occurrence and developmental pattern of neuromedin U-immunoreactive nerves in the gastrointestinal tract and brain of the rat. *Neuroscience* **25**: 797–816.

Bradford MM (1983) A rapid and sensitive method for the quantitation of microgram quantities of protein utilizing the principle of protein-dye binding. *Anal Biochem* **72**:248-253.

Brighton PJ, Szekeres PG, and Willars GB (2004) Neuromedin U and its receptors: structure, function, and physiological roles. *Pharmacol Rev* **56**: 231-248.

Cao CQ, Yu XH, Dray A, Filosa A, and Perkins MM (2003) A pro-nociceptive role of neuromedin U in adult mice. *Pain* **104**: 609-616.

Domin J, Ghatei MA, Chohan P, and Bloom SR (1987) Neuromedin U-a study of its distribution in the rat. *Peptides* **8**: 779-784.

Egecioglu E, Ploj K, Xu X, Bjursell M, Salome N, Andersson N, Ohlsson C, Taube M, Hansson C, Bohlooly M, Morgan D, and Dickson SL (2009) Central neuromedin U (NMU) signaling in body weight and energy balance regulation: Evidence from NMU receptor 2 deletion and chronic central NMU treatment in mice. *Am J Physiol* **296**: in press.

Fujii R, Hosoya M, Fukusumi S, Kawamata Y, Habata Y, Hinuma S, Onda H, Nishimura O, and Fujino M (2000) Identification of neuromedin U as the cognate ligand of the orphan G protein-coupled receptor FM-3. *J Biol Chem* **275**: 21068-21074.

Guan XM, Yu H, Jiang Q, Van Der Ploeg LH, and Liu Q (2001) Distribution of neuromedin U receptor subtype 2 mRNA in the rat brain. *Brain Res Gene Expr Patterns* **1**: 1-4.

Hanada R, Nakazato M, Murakami N, Sakihara S, Yoshimatsu H, Toshinai K, Hanada T, Suda T, Kangawa K, Matsukura S, and Sakata T (2001) A role for neuromedin U in stress response. *Biochem Biophys Res Commun* **289**: 225-228.

Hosoya M, Moriya T, Kawamata Y, Ohkubo S, Fujii R, Matsui H, Shintani Y, Fukusumi S, Habata Y, Hinuma S, Onda H, Nishimura O, and Fujino M (2000) Identification and functional characterization of a novel subtype of neuromedin U receptor. *J Biol Chem* **275**: 29528-29532.

Howard AD, Wang R, Pong SS, Mellin TN, Strack A, Guan XM, Zeng Z, D. L. Williams DL Jr. S.Feighner SD, Nunes CN, Murphy B, Stair JN, Yu H, Jiang Q, Clements MK, Tan CP, McKee KK, Hreniuk DL, McDonald TP, Lynch KR, Evans JF, Austin CP, Caskey CT, Van der Ploeg LH, and Liu Q (2000) Identification of receptors for neuromedin U and its role in feeding. *Nature* **406**: 70-74.

Kojima M, Haruno R, Nakazato M, Date Y, Murakami N, Hanada R, Matsuo H, and Kangawa K (2000) Purification and identification of neuromedin U as an endogenous ligand for an orphan receptor GPR66 (FM3). *Biochem Biophys Res Commun* **276**: 435-438.

Liu J, Hartman D, and Bostwick JR (2003) An immobilized metal ion affinity adsorption and scintillation proximity assay for receptor-stimulated phosphoinositide hydrolysis. *Anal Biochem* **318**: 91-99.

Marquette CA, and Blum LJ (2008) Electro-chemiluminescent biosensing. *Anal Bioanal Chem* **390**: 155-168.

Meng T, Su H, Binkert C, Fischli W, Zhou L, Shen J, and Wang M (2008) Identification of non-peptidic neuromedin U receptor modulators by a robust homogeneous screening assay. *Acta Pharmacol Sin* **29**: 517–527.

Miao W (2008) Electrogenerated chemiluminescence and its biorelated applications. *Chem Rev* **108**: 2506-2553.

Minamino N, Kangawa K, and Matsuo H (1985) Neuromedin U-8 and U-25: novel uterus stimulating and hypertensive peptides identified in porcine spinal cord. *Biochem Biophys Res Commun* **130**: 1078-1085.

Mori K, Miyazato M, Ida T, Murakami N, Serino R, Ueta Y, Kojima M, and Kangawa K (2005) Identification of neuromedin S and its possible role in the mammalian circadian oscillator system. *EMBO J* **24**: 325-335.

Nakahara K, Kojima M, Hanada R, Egi Y, Ida T, Miyazato M, Kangawa K, and Murakami N (2004) Neuromedin U is involved in nociceptive reflexes and adaptation to environmental stimuli in mice. *Biochem Biophys Res Commun* **323**: 615-620.

Raddatz R, Wilson AE, Artymyshyn R, Bonini JA, Borowsky B, Boteju LW, Zhou S, Kouranova EV, Nagorny R, Guevarra MS, Dai M, Lerman GS, Vaysse PJ, Branchek TA, Gerald C, Forray C, and Adham N (2000) Identification and characterization of two neuromedin U receptors differentially expressed in peripheral tissues and the central nervous system. *J Biol Chem* **275**: 32452-32459.

Sato S, Hanada R, Kimura A, Abe T, Matsumoto T, Iwasaki M, Inose H, Ida T, Mieda M, Takeuchi Y, Fukomoto S, Fujita T, Kato S, Kangawa K, Kojima M, Shinomiya K, and

Takeda S (2007) Central control of bone remodeling by neuromidin U. *Nat Med* **13**: 1234-1240.

Shan L, X. Qiao X, Crona JH, Behan J, Wang S, Laz T, Bayne M, Gustafson EL, Monsma FJ, Jr, and Hedrick JA (2000) Identification of a novel neuromedin U receptor subtype expressed in the central nervous system. *J Biol Chem* **275**: 39482-39486.

Szekeres PG, Muir AI, Spinage LD, Miller JE, Butler SI, Smith A, Rennie GI, Murdock PR, Fitzgerald LR, Wu H, McMillan LJ, Guerrera S, Vawter L, Elshourbagy NA, Mooney JL, Bergsma DJ, Wilson S, and Chambers JK (2000) Neuromedin U is a potent agonist at the orphan G protein-coupled receptor FM3. *J Biol Chem* **275**: 20247-20250.

Thompson EL, Murphy KG, Todd JF, Martin NM, Small CJ, Ghatei MA, and Bloom SR (2004) Chronic administration of NMU into the paraventricular nucleus stimulates the HPA axis but does not influence food intake or body weight. *Biochem Biophys Res Commun* **323**: 65-71.

Torres R, Croll SD, Vercollone J, Reinhardt J, Griffiths J, Zabski S, Anderson KD, Adams NC, Lori Gowen, Mark W. Sleeman MW, Valenzuela DM, Wiegand SJ, Yancopoulos GD, and Murphy AJ (2007) Mice genetically deficient in neuromedin U receptor 2, but not neuromedin U receptor 1, have impaired nociceptive responses. *Pain* **130**: 267-278.

Vigo E, Roa J, López M, Castellano JM, Fernandez-Fernandez R, Navarro VM, Pineda R, Aguilar E, Diéguez C, Pinilla L, and Tena-Sempere M (2007) Neuromedin S as novel putative regulator of luteinizing hormone secretion. *Endocrinol* **148**: 813-23.

Yu XH, Cao CQ, Mennicken F, Puma C, Dray A, O'Donnell D, Ahmad S, and Perkins M (2003) Pro-nociceptive effects of neuromedin U in rat. *Neuroscience* **120**: 467-474.

Zeng H, Gragerov A, Hohmann JG, Pavlova MN, Schimpf BA, Xu H, Wu L, Totoda H, Zhao M, Rohde AD, Gragerova G, Onrust R, Bergmann JE, Zhou M, and Gaitanaris GA (2006) Neuromedin U receptor-2-deficient mice display differential responses in sensory perception, stress, and feeding. *Mol Cell Biol* **26**: 9352-9363.

Zhang J, Chung TC, and Odenberger KR (1999) A simple statistical parameter for use in evaluation and validation of high throughput screening assays. *J Biomol Screen* **4**: 67-73.

Legends for Figures

Figure 1. ECL ligand binding assay with HEK293 cell membranes containing human NMUR2. **A**: the structure of $Ru(bpy)_3^{2+}$-labeled ligand; **B**: the saturation binding of $Ru(bpy)_3^{2+}$-NMU-23 to human NMUR2; **C**: the competition binding of unlabeled NMU-25, NMU-23 and NMU-8 in ECL binding assay using 0.5 nM $Ru(bpy)_3^{2+}$-NMU-23. The non-specific binding is defined by the binding in the presence of excess unlabeled NMU-8 (2 or 5 μM). Each data point is mean ± SD (n=5).

Figure 2. HTS with ECL ligand binding assay and identification of compounds that bind to human NMUR2. **A**: the scattergram of data from a representative 384-well plate. The 100% inhibition was defined by the effect of 1 μM NMU-8; **B**: the structures of PSOP, the most active compound identified from HTS (upper molecule), and the active enantiomer R-PSOP (lower molecule).

Figure 3. The activity of R-PSOP in binding to human NMUR2 in a radioactive competition binding assay using 0.2 nM [^{125}I] NMU-25 as labeled ligand. NMU-8 was used as an internal standard. Each data point is mean ± SD (n=5).

Figure 4. Concentration-dependent inhibition by R-PSOP of the PI turnover response in human NMUR2-expressing HEK293 cells stimulated by 10 nM NMU-25. The cells were pre-incubated with R-PSOP for 15 min followed by agonist stimulation for 45 min in the buffer containing 10 mM LiCl. Each data point is mean ± SD (n=3).

Figure 5. The functional activity of R-PSOP in calcium mobilization assay. **A**: Concentration-dependent stimulation of calcium mobilization response in HEK293 cells expressing human NMUR2 by NMU-25 in the presence of increasing concentrations of R-PSOP. The data were derived from FLIPR measurement of the maximal changes in fluorescence intensity and normalized to % activity based on the effect of 1 μM NMU-25. Each data point is mean ± SD (n = 4). **B**: Schild plot of the data from A. DR (dose ratio) is the ratio of the NMU-25 EC_{50} value in the presence of R-PSOP divided by the EC_{50} value in the absence of the antagonist.

Figure 6. The effects of R-PSOP on native receptors *in vivo*. NMU-23 (5 nmol intrathecally) produced an enhanced reflex response to pinch stimuli in decerebrate-spinal rats. This mechanical hypersensitivity was attenuated by R-PSOP (50 nmol intrathecally). Data are expressed as % change in number of action potentials evoked compared to baseline responses. The statistical significance of the differences were calculated between NMU-23-treated and vehicle group, as well as between the groups treated with NMU-23+R-PSOP *vs.* NMU-23 alone, by one-way ANOVA, *p<0.05, **p<0.01 and ***p<0.001. The arrows indicate the time point of NMU-23 or R-PSOP application.

JPET Fast Forward. Published on April 15, 2009 as DOI: 10.1124/jpet.109.152967
This article has not been copyedited and formatted. The final version may differ from this version.

Table 1. The *in vitro* pharmacological profile of R-PSOP in a broad selectivity screening. (A complete list of R-PSOP data on 104 targets is provided in the Supplemental Data file.)

	Target	Assay	Result	Reference compound
GPCR	Adrenergic α2a	[^{3}H]MK-912 binding	Inactive at 10 μM (n=3)	Yohimbine
	Cannabinoid CB1	[^{3}H]SR141716A binding	K_i>10 μM (n=3)	WIN55212-2
	Glutamate mGluR1	FLIPR calcium flux	Inactive at 10 μM (n=3)	LY341495
	Muscarinic m1	[^{3}H]NMS binding	K_i>10 μM (n=3)	Atropine
	Neurokinin NK1	[^{3}H]SR140333 binding	K_i>10 μM (n=3)	L-703606
	Opioid μ	[^{125}I]Enkephalin binding	K_i>10 μM (n=3)	Naloxone
	Serotonin 5-HT2A	[^{3}H]Ketanserine binding	Inactive at 10 μM (n=3)	Mianserine
Ion channel	$GABA_A$	[^{3}H]Flunitrazepam binding	Inactive at 10 μM (n=3)	Diazepam
	Sodium NaV1.3	Electrophysiology	IC_{50}>10 μM (n=3)	Tetrodotoxin
	Nicotinic AChR α7	[^{125}I]α-bungrotoxin binding	K_i=0.46 μM (n=4)	MLA
		Electrophysiology	EC_{50}=9.5 μM (n=2)	Nicotine
	Serotonin 5-HT_3	[^{3}H]GR-65630 binding	K_i = 0.22 μM (n=3)	MDL-72222
		Electrophysiology	EC_{50}=6.8 μM (n=2)	5-HT
Transporter	Norepinephrine transporter NET	[^{3}H]Nisoxetine binding	K_i>10 μM (n=3)	Reboxetine
Nuclear receptor	Estrogen ERα	[^{3}H]Estradiol binding	Inactive at 10 μM (n=3)	Diethylstilbestrol
Enzyme	Cholinesterase AChE	Enzymatic reaction	Inactive at 10 μM (n=3)	Physostigmine
	Monoamine Oxidase MAO_A	Enzymatic reaction	Inactive at 10 μM (n=3)	Clorgyline

JPET Fast Forward. Published on April 15, 2009 as DOI: 10.1124/jpet.109.152967
This article has not been copyedited and formatted. The final version may differ from this version.

Table 2. Pharmacokinetic properties of R-PSOP determined from rat *in vivo* studies. The values are mean ± SD.

Rat *i.v.* dosing at 5.2 μmol/kg (n=4)	
Area under curve (AUC)	1.1 ± 0.2 μM·hr
Clearance	76 ± 11 ml/min/kg
Half life ($t_{1/2}$)	2.2 ± 0.3 hr
Volume of distribution	10.2 ± 2.1 l/kg
Rat oral dosing at 12.1 μmol/kg (n=4)	
Area under curve (AUC)	0.14 ± 0.03 μM·hr
Clearance	1430 ± 270 ml/min/kg
Half life ($t_{1/2}$)	6.9 ± 0.5 hr
Bioavailability	2.6 ± 0.5%
Terminal studies: adult male rat *i.v.* dosing at 2.5 μmol/kg (n=6)	
Brain/plasma	0.18 ± 0.02
Spinal cord/plasma	0.38 ± 0.05
Maximal plasma level, C_{max}	1.2 ± 0.1 μM

JPET Fast Forward. Published on April 15, 2009 as DOI: 10.1124/jpet.109.152967
This article has not been copyedited and formatted. The final version may differ from this version.

Figure 1.

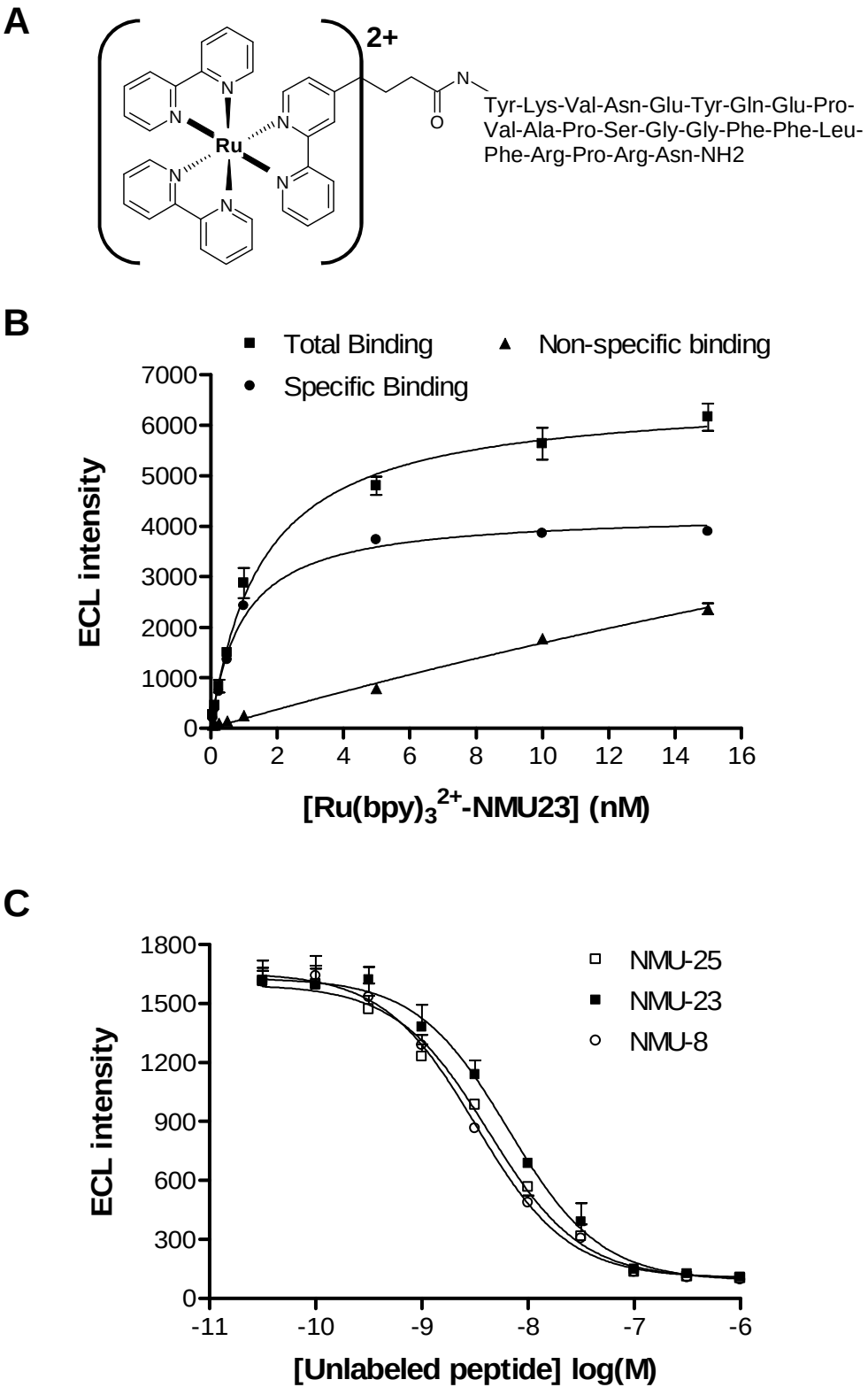

JPET Fast Forward. Published on April 15, 2009 as DOI: 10.1124/jpet.109.152967
This article has not been copyedited and formatted. The final version may differ from this version.

Figure 2.

A

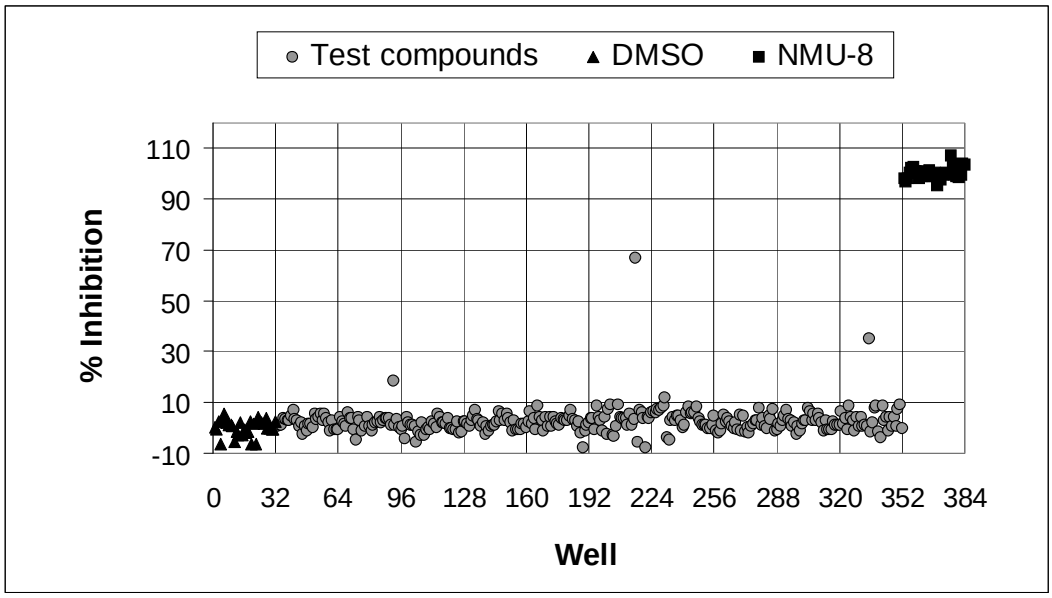

B

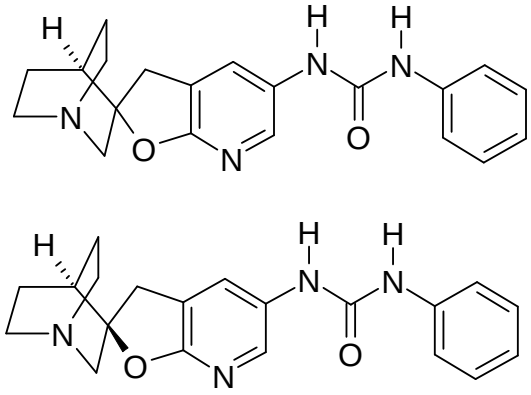

PSOP (upper) and R-PSOP (lower): (R)-5'-(Phenylaminocarbonylamino)spiro[1-azabicyclo[2.2.2]octane-3,2'(3'H)-furo[2,3-b]pyridine].

JPET Fast Forward. Published on April 15, 2009 as DOI: 10.1124/jpet.109.152967
This article has not been copyedited and formatted. The final version may differ from this version.

Figure 3

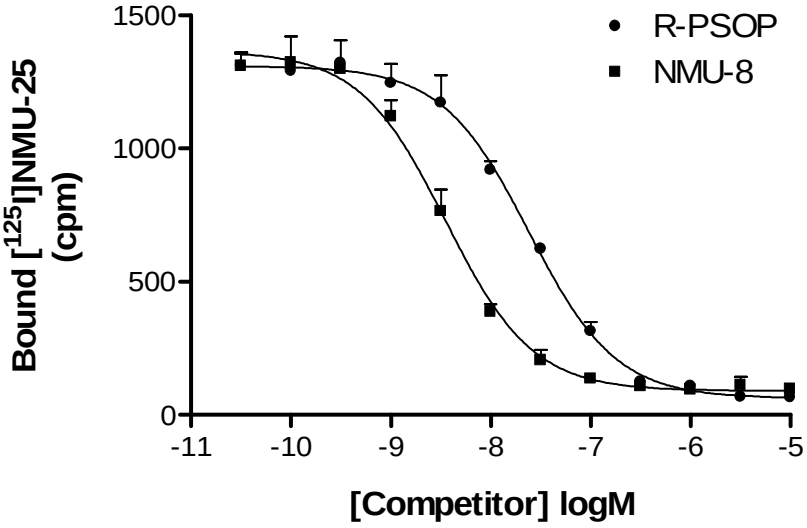

JPET Fast Forward. Published on April 15, 2009 as DOI: 10.1124/jpet.109.152967
This article has not been copyedited and formatted. The final version may differ from this version.

Figure 4.

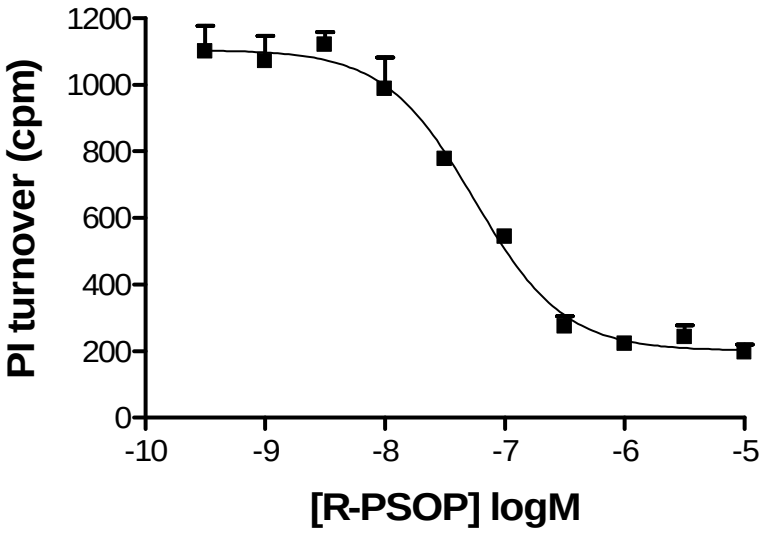

JPET Fast Forward. Published on April 15, 2009 as DOI: 10.1124/jpet.109.152967
This article has not been copyedited and formatted. The final version may differ from this version.

Figure 5.

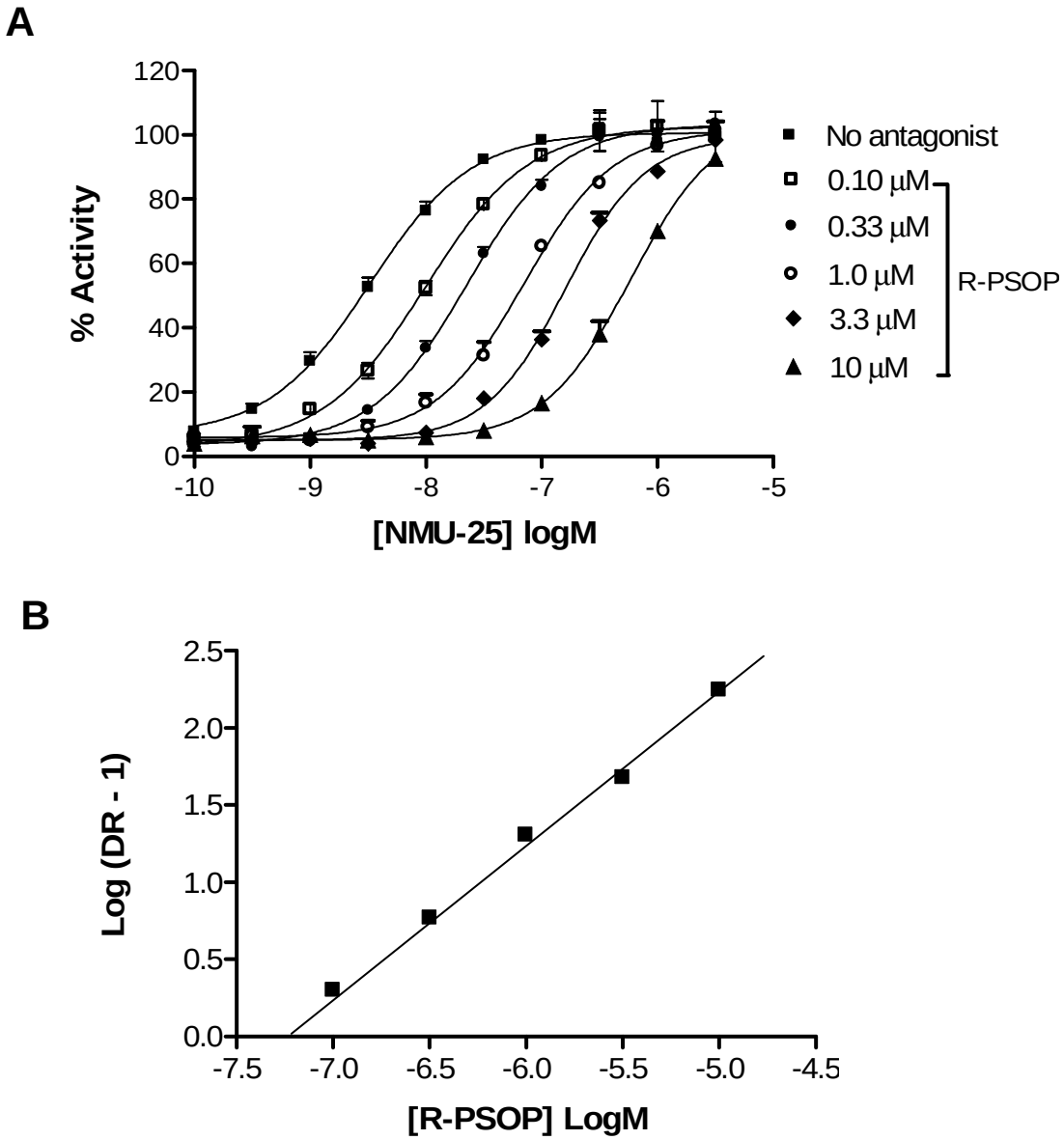

JPET Fast Forward. Published on April 15, 2009 as DOI: 10.1124/jpet.109.152967

Figure 6.